UC Berkeley

UC Berkeley Previously Published Works

Title

A microfluidic method for the selection of undifferentiated human embryonic stem cells and in situ analysis

Permalink

https://escholarship.org/uc/item/3nw9f0jt

Journal

Microfluidics and Nanofluidics, 18(5-6)

ISSN

1613-4982

Authors

Jabart, E
Rangarajan, S
Lieu, C
et al.

Publication Date

2015-05-01

DOI

10.1007/s10404-014-1485-9

Peer reviewed

eScholarship.org Powered by the California Digital Library
University of California

Author Manuscript

Author Manuscript

Author Manuscript

Author Manuscript

HHS Public Access

Author manuscript

Microfluid Nanofluidics. Author manuscript; available in PMC 2021 March 08.

Published in final edited form as:

Microfluid Nanofluidics. 2015 May ; 18(5-6): 955–966. doi:10.1007/s10404-014-1485-9.

A Microfluidic Method for the Selection of Undifferentiated Human Embryonic Stem Cells and *in Situ* Analysis

E. Jabart[1], **S. Rangarajan**[1], **C. Lieu**[2,a)], **J. Hack**[3], **I. Conboy**[1], **L. L. Sohn**[3,b)]

[1]Dept. of Bioengineering, University of California, Berkeley 94720, USA

[2]School of Medicine, Creighton University, Omaha, NE 68178, USA

[3]Dept. of Mechanical Engineering, University of California, Berkeley 94720, USA

Abstract

Conventional cell-sorting methods such as fluorescence-activated cell sorting (FACS) or magnetic-activated cell sorting (MACS) can suffer from certain shortcomings such as lengthy sample preparation time, cell modification through antibody labeling, and cell damage due to exposure to high shear forces or to attachment of superparamagnetic Microbeads. In light of these drawbacks, we have recently developed a label-free, microfluidic platform that can not only select cells with minimal sample preparation but also enable analysis of cells in situ. We demonstrate the utility of our platform by successfully isolating undifferentiated human embryonic stem cells (hESCs) from a heterogeneous population based on the undifferentiated stem-cell marker SSEA-4. Importantly, we show that, in contrast to MACS or FACS, cells isolated by our method have very high viability (~90%). Overall, our platform technology could likely be applied to other cell types beyond hESCs and to a variety of heterogeneous cell populations in order to select and analyze cells of interest.

Keywords

Human embryonic stem cells (hESCs); cell sorting; label-free; in situ analysis

1. INTRODUCTION

Conventional cell-sorting methods such as fluorescence-activated cell sorting (FACS) or magnetic-activated cell sorting (MACS) are often used to purify cells from heterogeneous populations using established cell-surface markers (Chapman et al., 2013; Jabart, Balakrishnan, & Sohn, n.d.; Lindström & Andersson-Svahn, 2010). Both FACS and MACS, however, can require large numbers of cells and, in some cases, adversely affect cells through either required exogenous labeling procedures or the use of high shear flows (as in the case of commercial FACS systems). Microfluidic-based FACS and MACS do not have such high shear flows, but they do suffer from lower throughput than their commercial counterparts. Examples of other adverse effects of FACS and MACS include cell death,

[b)]Author to whom correspondence should be addressed: sohn@me.berkeley.edu, 510-642-5434.
[a)]This research was performed while C. Lieu was at University of California, Berkeley, 94720

Author Manuscript Author Manuscript Author Manuscript Author Manuscript

modification of growth kinetics, or undesired initiation of cell signaling (Chapman et al., 2013; Didar & Tabrizian, 2010; C. Y. Fong, Peh, Gauthaman, & Bongso, 2009; Singh et al., 2013; Tárnok, Ulrich, & Bocsi, 2010). FACS and MACS are routinely utilized in sorting human embryonic stem cells (hESCs) (Eiges et al., 2001; C. Y. Fong et al., 2009; Hewitt et al., 2006; Schriebl et al., 2012; Sidhu & Tuch, 2006; Singh et al., 2013); however, there is a great interest in new sorting technologies for these particular cells and other cell types, given the aforementioned limitations of FACS and MACS.

hESCs are pluripotent cells, able to become any type of cell in the body (Thomson, 1998), and are a great potential source of cells for tissue engineering and regenerative medicine purposes. hESCs are a heterogeneous population of cells and selecting specific subpopulations could be important when considering therapeutic applications. In terms of new sorting technologies, one viable and obvious candidate for hESC sorting is microfluidics because of its ability to handle/process small sample volumes and the low shear forces to which samples are exposed. Few groups, however, have pursued this direction. Wang et al. used optical tweezers within a microfluidic device to sort OCT4-GFP+ hESCs (X. Wang et al., 2011). Dielectrophoretic methods could also be used to sort undifferentiated and differentiated hESCs based on differences in plasma membrane capacitance (Velugotla et al., 2012) and have been used to sort neuronal stem cells (Flanagan et al., 2008); however subsequent immunostaining or other methods are necessary to determine hESC subsets (e.g. $SSEA4^+$ cells). More recently, Singh et al. employed extracellular-matrix-coated microfluidic channels to sort undifferentiated and differentiated hESCs based on adhesion strength (Singh et al., 2013). They showed that microfluidics-sorted cells had >80% survival vs. FACS-sorted cells, which had only 40% survival.

Here, we showcase a low-shear, label-free, microfluidic platform for isolating a targeted sub-population of cells (in this case, hESCs) from a heterogeneous population. Cell mixtures are passed through an antibody-functionalized microfluidic channel: cells positive for the antibody target remain bound to the channel, while cells that are negative flow through the channel and are collected at the output. We demonstrate the broad utility of our method to sort different subpopulations of ESCs by utilizing different antibodies, such as SSEA-1, SSEA-4, and TRA-181. Through a Live/Dead® assay, we show that channel-bound cells that are subsequently collected have significantly higher viability (>20%) than those sorted with either MACS or FACS. Furthermore, for users who wish to perform secondary analysis of captured cells, we demonstrate our ability to analyze cells *in situ* by immunostaining the hESCs in-channel for a specific marker.

2. EXPERIMENTAL SECTION

2.1. Device fabrication

Figure 1A shows an image of our platform, which consists primarily of a polydimethylsiloxane (PDMS) mold permanently bonded to a glass substrate. The PDMS mold is created using standard soft-lithography techniques. Briefly, a silicon wafer is spin-coated with SU-8 2100 photoresist (3000 rpm for 30 sec), UV-exposed to a mask to pattern the resist, and then developed with SU-8 developer, thereby creating an 80-μm high negative-relief master. For the results we present here, we utilize the serpentine geometry

Author Manuscript Author Manuscript Author Manuscript Author Manuscript

shown in Figure 1B so that we increase the length of the channel and in turn, increase the possibility of a cell being captured. In general, however, our method is not limited to a serpentine channel, and a variety of channel geometries could be used. De-gassed Sylgard 184 (10:1 prepolymer:curing agent) is then poured onto the master wafer and cured at 80°C for 2 hours. The PDMS mold is then sliced and removed from the silicon master, cored at the inlet and outlet ports, exposed to oxygen plasma (200 mTorr, 80 W, 30 seconds), and bonded to a clean glass slide that is also exposed to oxygen plasma. The completed device is then heated to 150°C for 30 minutes to complete permanent bonding.

2.2. Device functionalization

Completed devices are initially filled with 1 M NaOH for 10 minutes, rinsed with 18 MΩ de-ionized (DI) water, and dried on a hotplate for 10 minutes at 150°C. The glass surface enclosed by the microfluidic channel is silanized in a humid chamber using N-(3-triethoxysilylpropyl)-4-hydroxybutyramide (Gelest, Morrisville, PA), diluted in a stock solution of 0.01% acetic acid in 95% ethanol and 5% DI water for 4 hours at room temperature (RT), as done previously (Carbonaro, Mohanty, Huang, Godley, & Sohn, 2008; Chapman et al., 2013). Channels are then rinsed with stock solution and DI water and subsequently dried and cured for 2 hours at 120°C. Silane-coated serpentine channels are incubated with the homo-bifunctional amine crosslinker sulfo-EGS (Pierce, Rockford, IL) at 3 mg/mL in PBS for 20 minutes at RT. Protein G (1.00 mg/mL) or Protein L (1.66 mg/mL) (Pierce) (both of which are regularly used for antibody binding) (Akerstroms & Bjork, 1989; De Château et al., 1993; Vered Bronner, Moran Tabul, 2009) is then crosslinked to the silanized surface by incubation for 4 hours in a humid chamber. Finally, antibodies (SSEA-1, SSEA-4, mouse IgG_3, mouse IgM, Tra-1–81 – all obtained from Biolegend, San Diego, CA), diluted to 1.33 μM for IgG isotype antibodies (which are bound by Protein G) and to 556 nM for IgM isotype antibodies (undiluted stock concentration, which are bound by Protein L), are linked to the surface by overnight incubation at 4°C. This entire functionalization procedure provides antibody immobilization stability over an extended period of time, as previously demonstrated (Balakrishnan et al., 2013; Chapman et al., 2013; Jabart et al., n.d.)

2.3. COMSOL modeling of shear rates in microchannel

The shear rates in the microfluidic channel were modeled using the COMSOL microfluidics module (COMSOL Inc., Palo Alto, CA). Laminar flow was assumed, and the channel was simulated using input flow rates of 2, 5, and 10 μL/min. Since shear increases closer to the edges of the microchannel (within the first 10 μm), the mesh resolution was selected in order to highlight the effects in the boundary layer.

2.4. Cell Culture

2.4.1. hESCs—H9 human embryonic stem cells (hESCs) (WiCell Research Institute, Madison, WI) were cultured on BD Matrigel hESC-qualified Matrix (BD Biosciences, San Jose, CA) in mTeSR1 basal medium with 5X supplement (STEMCELL Technologies, Vancouver, Canada). Cells were routinely passaged, as per the manufacturer's protocol. For single-cell dissociation of colonies, H9s were washed briefly with PBS, incubated at 37°C

Author Manuscript Author Manuscript Author Manuscript Author Manuscript

for 12 minutes with 2 mM EDTA in PBS (Invitrogen, Carlsbad, CA), and gently triturated. Cells were sedimented and re-suspended as single cells in fresh medium before passing through the microchannels (final concentration 2,000–2,500 cells/μL).

2.4.2. A549s—A549 lung carcinoma cells (ATCC, Manassus, VA) were cultured in DMEM supplemented with 10% FBS and 1 X penicillin/streptomycin and routinely passaged, as per the manufacturer's protocol. A549s were dissociated by treatment with 0.25% trypsin/EDTA for 3 min at 37°C, neutralized with media, sedimented, and re-suspended at 500 cells/μL before passing through microchannels.

2.4.3. mESCs—Murine embryonic stem cells (J1 mESCs: J1s, ATCC # SCRC-1010) previously maintained on a murine embryonic fibroblast layer were cultured for 3–4 passages on 0.1% gelatin (in PBS) in DMEM (high glucose) (Invitrogen, Carlsbad, CA), supplemented with 2 mM GlutaMAX-I Supplement (Invitrogen), 1 mM MEM Sodium Pyruvate Solution (Invitrogen), 0.1 mM MEM Non-Essential Amino Acids Solution (Invitrogen), 1 X penicillin/streptomycin Dual Antibiotic Solution (Fisher, Pittsburgh, PA), 55 μM 2-Mercaptoethanol (Invitrogen), 15% FBS (KO SR, Invitrogen) and 1000 U/mL ESGRO LIF (Millipore, Billerica, MA). mESCs were dissociated into single cells by incubation with 0.25% trypsin/EDTA for 3 minutes at 37°C, sedimented, and re-suspended at 2,500 cells/μL before passing through prepared microchannels.

2.5. Device operation

Because antibodies require longer times to reach equilibrium at 4°C vs. 37°C and because antibody-antigen dissociation kinetics are limited at room temperature, we operated our devices at room temperature (Reverberi & Reverberi, 2007). Thus, antibody-functionalized microchannels were brought to RT, rinsed once with PBS, and then equilibrated in the appropriate media for 30 minutes. Homogeneous or heterogeneous cell populations were diluted to 2,500 cells/μL in their respective media at an equal ratio to the cell distribution (e.g. a 4:1 mixture of hESCs: A549s contained 2,000 cells/μL hESCs and 500 cells/μL A549s in 80% mTeSR1/20% DMEM media). 35 μL of the cell suspension (~87,500 cells) flowed through the channels at 2 μL/min via a syringe pump and collected for further analysis (Figure 1B). The channels were then washed with 15 μL of media at 5 μL/min and then 30 μL of media at 10 μL/min to remove unbound cells. A LabSmith SVM340 Synchronized Video Microscope allowed white-light visualization of the microfluidic device to confirm that all unbounded cells had been removed.

2.6. Immunostaining

To confirm the success of our sorting, we performed immunostaining on the cells. In particular, control cells (i.e. cells that did not run through the channels), channel flow-through cells, and channel-bound hESCs were immunostained for SSEA-4 and OCT4, two markers of undifferentiated stem cells. Briefly, cells were washed once with PBS, fixed for 15 minutes at RT in 4% paraformaldehyde, washed three times, 5 minutes each, with staining buffer (SB: 1% bovine growth serum, 1 mg/mL sodium azide in 1X PBS), permeabilized (for internal staining only) with 0.25% Triton X-100 in SB, washed three times 5 minutes each in SB, and labeled with primary antibodies for 2–4 hours at RT or

Author Manuscript Author Manuscript Author Manuscript Author Manuscript

overnight at 4°C at manufacturer-recommended dilutions. Cells were then washed 3 times, 5 minutes each, with SB, incubated for one hour in the dark at RT with fluorophore-conjugated secondary antibodies (Molecular Probes) and Hoechst at 2 μM, washed three times, 5 minutes each, with SB, and either imaged (for the in-channel staining) or mounted with Fluoromount (Sigma-Aldrich, St. Louis, MO) for imaging. Images were taken using a fluorescent microscope.

2.7. MACS

J1 mESCs were sorted using MACS anti-IgM or anti-SSEA-1 Microbeads (Miltenyi, Auburn, CA). Following the manufacturer's protocol for MACS preparation, single-cell J1s were centrifuged at 300 g for 10 minutes and re-suspended in 80 μL of MACS buffer per 10^7 cells (or the total amount of cells if less than 10^7). 20 μL of anti-IgM or anti-SSEA-1 Microbeads were then added and incubated with the cells for 15 minutes at 4°C. The cells were then washed twice with 2 mL of MACS Buffer and re-suspended in 500 μL of MACS Buffer. After magnetic-column preparation, cells were added. Flow-through cells were collected by gravity; bound cells were collected by manually applying pressure via a 5 mL syringe plunger. A Live/Dead® viability assay was immediately performed with the collected cells (see Viability assay).

2.8. FACS

FACS for the SSEA-1 antigen on J1 mESCs was completed using established protocols for indirect immunofluorescence (Abcam, n.d.). J1 mESCs were washed and incubated with 0.25% trypsin/EDTA for 3 min at 37°C, washed with PBS, and re-suspended in a PBS solution with 10% FBS at a concentration of 10^6 cells/mL. 100 μL of the suspension was incubated with either anti-SSEA-1 or the corresponding IgG control antibody for 30 minutes at RT. The suspension was then collected and washed 3 times with PBS by centrifugation at 400 g for 5 minutes and resuspended in the PBS solution with 10% FBS. Cells were then incubated with fluorescently-labeled secondary antibodies for 30 minutes at RT in the dark to avoid fluorophore photobleaching, and again washed 3 times with PBS for 5 minutes each. On the final wash, cells were resuspended in PBS and collected for FACS. Although higher cell viability is often achieved by keeping cells on ice during a staining procedure, we did not observe any negative effects by staining at RT. In fact, attempts to stain cells on ice led to poor fluorescent signal, which was increased only upon staining at RT.

J1 mESCs were sorted in a MoFlo Legacy (2002) high-performance cell sorter (Beckman Coulter, Miami, FL) equipped with a Coherent Inc. Innova 90 argon ion-gas laser (Santa Clara, CA) tuned for 488 nm light emission and running at 200 mW. PE fluorescence was directed to a PMT detector using a 605 nm dichroic short pass filter and a 555 nm dichroic long-pass to a 580 nm band-pass optical filter with a bandwidth of 30 nm (Omega Optical, Brattleboro, VT). The MoFlo cell sorter ran at a pressure of 50 psi with a 70 μM flow-cell tip. Samples were maintained at 4°C while being sorted.

2.9. Viability assay

Unsorted and sorted (via MACS, FACS, or microchannel) mESCs were analyzed by Live/Dead® Assay (Invitrogen, Carlsbad, CA), per the manufacturer's protocol and as previously

Author Manuscript Author Manuscript Author Manuscript Author Manuscript

described(Abruzzese & Fekete, 2013; Holm, 2012; Hwang, Varghese, & Elisseeff, 2007; Liu et al., 2010; Liu, Judd, & Lakshmipathy, 2013; Quinlan, 2006). Collected cells from each assay were sedimented by centrifugation for 5 minutes at 300 g, washed once with PBS for 5 minutes, spun again for 5 minutes at 300 g, and re-suspended in 1 mL of PBS. A 150 μL aliquot of cells was then allowed to settle briefly on a cover slip. 150 μL of Live/Dead® reagent (2 μM calcein AM and 4 μM ethidium homodimer 1 in PBS) was added to the cover slip and incubated in the dark for 45 minutes at RT. The cover slip was then flipped onto a glass slide and imaged as previously described. Live (green) and dead (red) cells were counted. Over 2000 cells were counted in each case. For FACS-sorted cells, distinguishing dead cells (ethidium homodimer 1, red) vs. SSEA-1-labeled cells (PE) was readily achieved based on the greater intensity of the fluorescent signal for dead cells, the clear nuclear localization of the signal, and the absence vs. presence of green fluorescence (Figure 4, appendix).

3. RESULTS

3.1. Flow-through and bound cells from anti-SSEA-1 Microbeads show decreased survival

Figure 2A shows the effects of MACS sorting on mESC cell viability. Cells from the anti-IgM Microbead flow-through showed no significant decrease in viability after MACS sorting. Intriguingly, cells incubated with anti-SSEA-1 Microbeads, whether from the flow-through or the bound fraction, showed a significant (31% and 26%, respectively) decrease in cell survival as compared to the control condition in repeated experiments.

3.2. SSEA-1-labeled cells also show a decrease in survival via FACS

Figure 2B shows the percentage of cell survival after FACS normalized to unsorted cells maintained in media. Cells incubated with IgM or cells negative for SSEA-1 that had been incubated with anti-SSEA-1 antibodies and sorted by FACS showed a small decrease in viability (16% and 12%, respectively). Our results are consistent with published literature on the poor ESC cell survival after FACS sorting (Emre et al., 2010; Singh et al., 2013). However, SSEA-1^+ cells labeled with anti-SSEA-1 antibodies and sorted by FACS had nearly a 45% decrease in cell survival as compared to the control cells maintained in media. This decrease in cell viability might be explained by the possible negative effects of antibody binding in combination with the prolonged time the cells spend in suspension before analysis. (Chapman et al., 2013; Didar & Tabrizian, 2010; C.-Y. Fong, Gauthaman, & Bongso, 2010; Jabart et al., n.d.; Toh & Voldman, 2011).

3.3. Positively-selected cells show increased survival

Both MACS and FACS showed decreases (26% and 44%, respectively) in the survival of SSEA-1-selected cells (as compared to ~90–100% viability of cells analyzed with control IgM). In contrast, positively-selected cells in our serpentine channel (i.e. collected cells that bound anti-SSEA-1 microchannels) showed ~90% viability as compared to control cells that did not run through the channels or cells analyzed with IgM. Interestingly, cells that flowed through the SSEA-1 microchannels without binding were only ~55% viable (Figure 2C), indicating that the anti-SSEA-1 channels did preferentially bind viable cells. Clearly, some

Author Manuscript Author Manuscript Author Manuscript Author Manuscript

cell death occurs in our microfluidic channels, since both the bound and flow-through populations have lower viability than the starting cells. The decrease in viability of cells that run through the anti-SSEA-1 microchannels may be partially attributed to the capture of live cells by the anti-SSEA-1 antibodies; however, further investigation is necessary to determine all the sources that contribute to this lower viability. Such investigation includes focusing on the total number of viable cells captured in the channels vs. those collected at the output and determining to what extent flowing cells through an anti-SSEA-1 channel is more detrimental to viability than running through control IgM channels. Nonetheless, the important result here is that the viability of positively-selected cells in the channel is very high and greater than that using either FACS or MACS, neither of which focus on the preferential selection of viable cells.

3.4. Improved capture of hESCs with anti-SSEA-4-functionalized channels

When mixed populations of 4:1 hESCs and A549s were passed through anti-SSEA-4-functionalized channels, >90% of the cells captured in the channel were SSEA-4^{+}, as confirmed by in-channel staining of either OCT4 or SSEA-4 (Figure 5, appendix). The SSEA-4 expression was similar to stained control hESCs (data not shown). The percentage of hESCs in the mixed population prior to passing through the microchannels was compared to the percentage of hESCs in the cell population collected in the output (either through IgG- or anti-SSEA-4-coated channels), based on either SSEA-4 or OCT4 expression. This difference was normalized over the various runs to generate Figures 3A and B. Overall, we demonstrate a 60% reduction in the number of hESCs in our mixed population. Improvements in cell capture could increase this efficiency. A visual inspection of all the isotype control antibody channels showed that no cells bind at any time during sorting. Thus, binding in the specific antibody channels is indeed based on specific interactions between the SSEA-4 antibodies and the hESC cell-surface SSEA-4 antigen.

3.5. Capture of hESCs with anti-Tra-1–81-functionalized channels

To show the generality of our technique and the flexibility to sort cells based on a wide-array of receptor expression, hESCs were mixed at a 4:1 ratio with A549 cells and passed through serpentine channels functionalized with anti-Tra-1–81, another marker of undifferentiated hESCs. Cell mixtures were immunostained for the undifferentiated hESC marker OCT4 and the percent of hESCs in the pre-channel and post-channel cell populations was determined. As shown in Figure 3C, only a 32% reduction in the percentage of hESCs was obtained using Tra-1–81. This lower capture efficiency is explained in Discussion.

3.6. Shear rate modeling in microchannels using COMSOL

Shear rates in the device were modeled using COMSOL (Figure 6, appendix). At our running flow rate of 2 μL/min, the average shear rate was 14.9 s^{-1}, increasing up to 37.3 s^{-1} at 5 μL/min and to 74.6 s^{-1} at 10 μL/min during washes. At 2 μL/min, the shear rate increases to 27 s^{-1} for cells along the edges of the device; in the curves, the shear rate ranges from 21 s^{-1} to 36 s^{-1} from the exterior to the interior. Likewise, at 5 μL/min, the peak shear rate is 91 s^{-1} toward the interior of the curves; at 10 μL/min, the maximum is 183 s^{-1}. The shear rates experienced by cells are all on the lower end of what are typically experienced in microcirculation (McCarty, Jadhav, Burdick, Bell, & Konstantopoulos, 2002).

Author Manuscript Author Manuscript Author Manuscript Author Manuscript

4. DISCUSSION

FACS and MACS with commercial instruments have long been the standard for numerous cell-sorting applications. However, their associated constraints – the preference for large numbers of cells, exogenous labeling, high-shear stresses, high cost (for FACS), and interaction with superparamagnetic Microbeads (for MACS) – have paved the way for microfluidics to address cell sorting in novel ways. The microfluidic method we described here can be used to positively select cells from a mixed population. Moreover, our method requires little sample preparation, as cells can be sorted under low shear forces, without any labeling, and depending on the user's needs or preferences, to be either analyzed *in situ* by immunostaining in the microchannel or retrieved for subsequent analysis.

Our microfluidic method provides a number of advantages over conventional sorting methods such as FACS and MACS. Once cells are dissociated into single cells, they are ready to be injected into the device. Unlike FACS and MACS, sample preparation does not require direct labeling of cells with antibodies or superparamagnetic Microbeads. The only preparation involved is dissociating and collecting the cells, a step common to all three sorting methods. Operating two microchannels simultaneously takes only 30 minutes, with only 30 minutes of cell sample preparation time, as just described; for MACS, cell labeling with Microbeads takes up to 1.5 hours, followed by over an hour of sorting; for FACS, cell preparation time can take up to 2 hours followed by 2 hours of sorting, which includes required setup and gating. The percentage of live cells retrieved after being captured in our device (~90%) is also greater than that achieved with either MACS or FACS (75% and 55%, respectively), suggesting a gentler treatment of cells. This is an especially important feature when there is a need to sort/isolate cells which are few in number or are negatively affected by lengthy processing times in suspension. Moreover, our device also allows for further *in situ* analysis of selected bound cells (e.g. in-channel staining for cell-surface markers) should the user desire this. Although MACS and FACS have greater throughput, running parallel arrays of prepared microfluidic channels could greatly augment throughput of our method. In addition, in situations where cell numbers are limited and starting populations are minute (e.g. analysis of ESC populations from pre-implantation embryos), our microfluidic-based cell isolation and analysis could become very valuable.

4.1. Selected cell capture with anti-Tra-1–81 vs. anti-SSEA-4-functionalized channels

Both Tra-1–81 and SSEA-4 are expressed in hESCs (Draper, Pigott, Thomson, & Andrews, 2002; Qiu et al., 2008; Zhao, Ji, Zhang, Li, & Ma, 2012). However, as shown in Figure 3, the anti-Tra-1–81 channels show a decreased efficiency in hESC capture. This decrease may be explained by the combination of several factors including decreased antibody surface density, and less favorable antigen-binding-site display – both of which are correlated with the antibody isotype used for functionalization – or heterogeneity of hESC surface-marker expression and localization of receptors on the cell surface.

To understand the effects of antibody surface density on capture efficiency, we estimated the functionalized-antibody density in the channels, N_{Ab} (Carbonaro et al., 2008; Cozens-Roberts, Quinn, & Lauffenberger, 1990) to be,

Author Manuscript Author Manuscript Author Manuscript Author Manuscript

$$N_{Ab} = 0.7[Ab]V_p\left(\frac{A_v}{A_p M_w}\right)$$

where $[Ab]$ is the antibody concentration used to functionalize the channels, V_p is the total channel volume, A_v is Avogadro's number, A_p is the total glass surface area that is functionalized, and M_w is the molecular weight of the antibody. As previously described by Cozens-Roberts et al. (1990) and Clausen (1981), we also assume that only 70% of antibodies bind to the surface (Clausen, 1981; Cozens-Roberts et al., 1990). For the channels functionalized with IgG-isotype antibodies and IgM-isotype antibodies, we therefore obtain $N_{Ab} \sim 4.5 \times 10^4$ antibodies/μm^2 and $N_{Ab} \sim 1.87 \times 10^4$ antibodies/μm^2, respectively. Considering that IgG antibodies and IgM antibodies have a hydrodynamic radius of 5.29 nm and 12.65 nm, respectively(Armstrong, Wenby, Meiselman, & Fisher, 2004), then the maximum theoretical antibody coverage we could obtain in a single antibody layer would be 1.14×10^4 antibodies/μm^2 and 1.99×10^3 antibodies/μm^2, respectively. We are therefore functionalizing our devices at saturating concentrations. In addition, based on these calculations, we estimate that IgM-isotype-functionalized channels have ~6-fold fewer antibodies than their IgG-isotype-functionalized counterparts. Although IgM-isotype antibodies have 5-times more antigen-binding sites than their IgG counterparts, not all sites will bind cells thereby reducing the capture efficiency in the anti-Tra-1–81 channels (IgM-isotype).

In regards to the effects of antigen-binding-site display, the functionalization differences between IgG- and IgM-isotype antibodies may also contribute to reduced capture efficiency. In the functionalization strategy, IgG-isotype antibodies (such as SSEA-4) were conjugated to the surface via Protein G, which has two Fc-binding domains. The SSEA-4 antigen-binding sites, which are far from the Fc region, are then free to bind SSEA-4 receptors on the hESCs. For the IgM-isotype antibodies (such as Tra-1–81), Protein L has four immunoglobulin-binding domains per protein. However, Protein L interacts with the kappa light chain on antibodies, which is closer to the antigen-binding site than the Fc region. The IgM antibodies, pentamers of IgGs, which have a significantly larger hydrodynamic radius (12.65 nm as compared to 5.29 nm for IgG) (Armstrong et al., 2004) may then present a less favorable display of the binding sites for Tra-1–81 on hESCs, and consequently contribute to our lower capture efficiency.

Although undifferentiated hESC markers are well-characterized, it is also clear that there exists significant heterogeneity between hESC lines and even within pluripotent hESC populations from the same line with respect to the levels of expressed proteins (Gu et al., 2010; Mantel et al., 2007; Qiu et al., 2008; Stewart et al., 2006). Pluripotent hESCs have the potential to become any type of cell in our body, but all pluripotent cells may not have the same expression level of the various stem-cell markers (Stewart et al., 2006). For example, Qiu et al. (2008) demonstrated that expression of Tra-1–81 receptors varies significantly even among stem cells from the same line (Qiu et al., 2008). Future experiments to determine expression level of receptors on the surface could help determine whether this as a potential source of the difference in capture efficiency.

Author Manuscript Author Manuscript Author Manuscript Author Manuscript

4.2. Antibody-functionalized microfluidic devices

Several recent papers have addressed the topic of using antibody-functionalized microdevices for isolating specific sub-populations from a heterogeneous population (Didar & Tabrizian, 2010; Mittal, Wong, Deen, & Toner, 2012). Isolating specific immune cells or rare cells such as circulating tumors cells are among the most common applications (Alix-Panabières & Pantel, 2014; Murthy, Sin, Tompkins, & Toner, 2004; Nagrath et al., 2007; Plouffe, Kniazeva, Mayer, Murthy, & Sales, 2009; Pratt, Huang, Hawkins, Gleghorn, & Kirby, 2011; Sekine, Revzin, Tompkins, & Toner, 2006). Three main challenges arise when designing antibody-based capture microdevices: directing cells to the antibody-coated surface, increasing the effective area of interaction, and designing with shear-stress considerations.

In microchannels with no mixing, cells will, over time, move more and more along streamlines. If these streamlines do not promote cell interaction with the antibody-functionalized surface, then the amount of time cells are able to spend interacting – and potentially binding – to functionalized antibodies decreases, thus decreasing the overall capture efficiency (Cheng et al., 2007; Mittal et al., 2012). Our microchannels most likely suffers from this situation as most binding was observed early on in the device, progressively decreasing as cells moved farther along into the channel (despite our intention and use of a “serpentine” channel geometry). In addition, as cells move through the microchannel and fail to interact with the antibody-coated surface, we observed cells beginning to clump, further decreasing the possibility of capture. In order to increase cell-antibody interactions, one could incorporate a herringbone design to promote mixing (Mittal et al., 2012; Stott et al., 2010; S. Wang et al., 2011), or could increase the effective surface area, for example, by incorporating antibody-functionalized microposts in addition to a functionalized solid surface (Gleghorn et al., 2010; Nagrath et al., 2007; S. Wang et al., 2009).

The capture efficiency of our device could be improved on several fronts. Running collected cells through a second or multiple rounds of devices should be a straightforward method to improved capture efficiency. Control of the presentation of antibodies, such as their orientation, the amount of surface coverage, or selection of antibodies with greater affinity, can promote cell-antibody interactions and cell rolling (Cheung et al., 2011; Zheng, Cheung, Schroeder, Jiang, & Zohar, 2011), ultimately leading to increased cell capture (Myung, Launiere, Eddington, & Hong, 2010). While we do partially control antibody orientation via Protein G, including some of the aforementioned modifications (e.g. flow control to induce mixing/increase cell-antibody interaction or increasing effective surface area with microposts) should boost the capture efficiency of our device.

5. CONCLUSION

We demonstrate a design of an antibody-functionalized PDMS microfluidic channel that is capable of positively selecting cells from a mixed population for *in situ* immunofluorescence or subsequent retrieval and analysis of cells with high viability. To our knowledge, this is the first time antibody-functionalized microchannels have been used to capture hESCs. The use of a microfluidic device with the ability to isolate cells such as hESCs with short sample preparation time, low shear stress, and no labeling, provides a platform technology with

Author Manuscript Author Manuscript Author Manuscript Author Manuscript

certain advantages over FACS and MACS. With improved capture efficiency, these devices could allow for isolating cell populations that would not be feasible with FACS or MACS (e.g. low cell numbers, sensitive cell samples) and for analyzing bound single cells *in situ*.

ACKNOWLEDGMENTS

We would like to thank the Siebel Scholars Foundation for their support of E.J. and the W. M. Keck Foundation, California Institute for Regenerative Medicine CIRM RN1-0032, and NIH/NIA AG 027252 for partial support of this work. We thank M. Mir, K. Balakrishnan, W. Cousin, and C. Elabd for a critical reading of this manuscript and helpful comments.

APPENDIX – SUPPORTING FIGURES

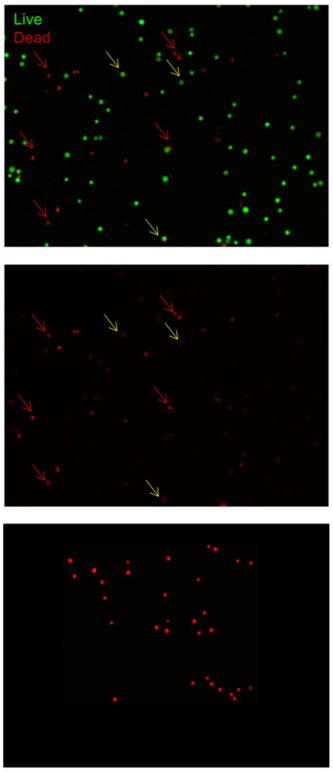

Fig.4.

Fluorescent images of Live (green) / Dead (red) cells after SSEA-1^+ FACS sorting. Cells labeled with PE (yellow arrows) show only faint, background fluorescence, along the cell membrane and are robustly green, i.e. live, whereas dead cells (red arrows) are bright and nuclear stain is clear, while the green, live signal is undetectable. The dead cell control image shows that ethidium homodimer 1 stained cells (red) do not have background levels of staining and are always bright and nuclearly-stained

Author Manuscript Author Manuscript Author Manuscript Author Manuscript

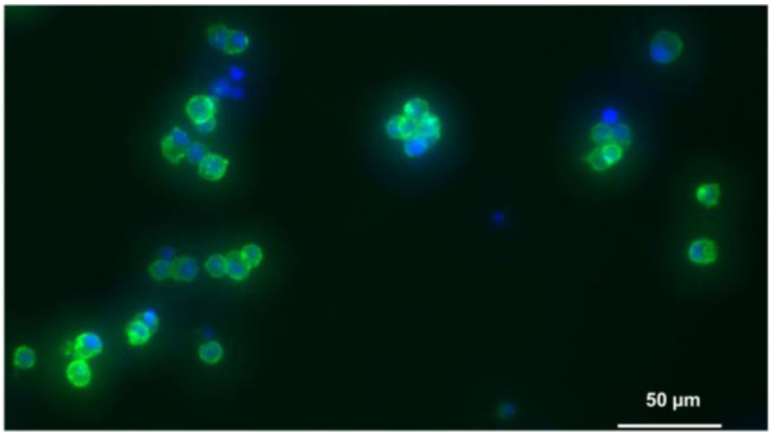

Fig.5.
hESCs bound inside an anti-SSEA-4-functionalized channel were stained for SSEA-4 (green) and Hoechst (blue). More than 90% of cells stained positive for SSEA-4

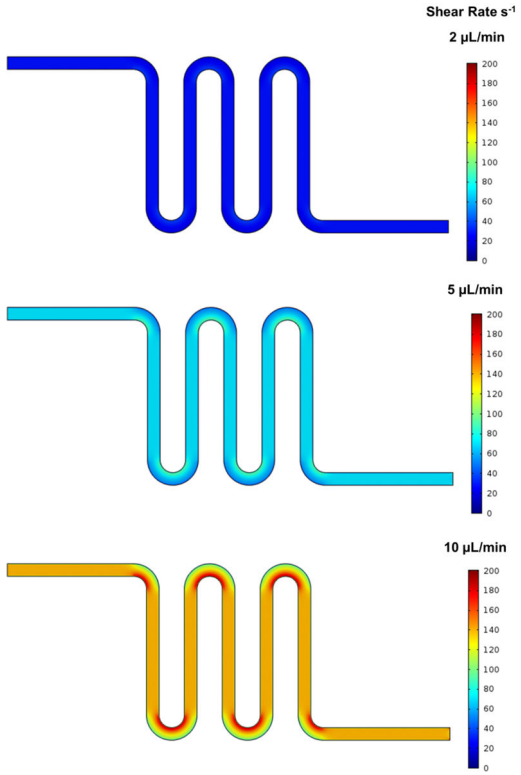

Fig.6.
COMSOL-modeled shear rates in the microfluidic device at the running flow rate of 2 µL/min and the two washing flow rates, 5 µL/min and 10 µL/min

REFERENCES

Abcam. (n.d.). Indirect flow cytometry (FACS) protocol. Retrieved from http://www.abcam.com/index.html?pageconfig=resource&rid=11381

Author Manuscript Author Manuscript Author Manuscript Author Manuscript

Abruzzese RV, & Fekete RA (2013). Chapter 17 Single Cell Gene Expression Analysis of Pluripotent Stem Cells. In Pluripotent Stem Cells (Vol. 997, pp. 217–224). doi:10.1007/978-1-62703-348-0

Akerstroms B, & Bjork L (1989). Protein L : An Immunoglobulin Light Chain-binding Bacterial Protein, 264(33), 19740–19746.

Alix-Panabières C, & Pantel K (2014). Technologies for detection of circulating tumor cells: facts and vision. Lab on a Chip. doi:10.1039/c3lc50644d

Armstrong JK, Wenby RB, Meiselman HJ, & Fisher TC (2004). The hydrodynamic radii of macromolecules and their effect on red blood cell aggregation. Biophysical journal, 87(6), 4259–70. doi:10.1529/biophysj.104.047746 [PubMed: 15361408]

Balakrishnan KR, Anwar G, Chapman MR, Nguyen T, Kesavaraju A, & Sohn LL (2013). Node-pore sensing: a robust, high-dynamic range method for detecting biological species. Lab on a chip, 1302–1307. doi:10.1039/c3lc41286e [PubMed: 23386180]

Carbonaro A, Mohanty SK, Huang H, Godley LA, & Sohn LL (2008). Cell characterization using a protein-functionalized pore. Lab on a Chip, 8, 1478–1485. Retrieved from http://www.ncbi.nlm.nih.gov/pubmed/18818802 [PubMed: 18818802]

Chapman MR, Balakrishnan KR, Li J, Conboy MJ, Huang H, Mohanty SK, … Sohn LL (2013). Sorting single satellite cells from individual myofibers reveals heterogeneity in cell-surface markers and myogenic capacity. Integrative biology quantitative biosciences from nano to macro, 692–702. doi:10.1039/c3ib20290a [PubMed: 23407661]

Cheng X, Irimia D, Dixon M, Sekine K, Demirci U, Zamir L, … Toner M (2007). A microfluidic device for practical label-free CD4(+) T cell counting of HIV-infected subjects. Lab on a Chip, 7, 170–178. Retrieved from http://www.ncbi.nlm.nih.gov/pubmed/17268618 [PubMed: 17268618]

Cheung LS-L, Zheng X, Wang L, Baygents JC, Guzman R, Schroeder J. a, … Zohar Y (2011). Adhesion dynamics of circulating tumor cells under shear flow in a bio-functionalized microchannel. Journal of Micromechanics and Microengineering, 21(5), 054033. doi:10.1088/0960-1317/21/5/054033

Clausen J (1981). Laboratory Techniques in Biochemistry and Molecular Biology, Vol. 1 (Work TS.). North-Holland Publishing Co., New York.

Cozens-Roberts C, Quinn JA, & Lauffenberger DA (1990). Receptor-mediated adhesion phenomena. Model studies with the Radical-Flow Detachment Assay. Biophysical Journal, 58, 107–125. Retrieved from http://www.pubmedcentral.nih.gov/articlerender.fcgi?artid=1280944&tool=pmcentrez&rendertype=abstract [PubMed: 2166596]

De Château M, Nilson BH, Erntell M, Myhre E, Magnusson CG, Akerström B, & Björck L (1993). On the interaction between protein L and immunoglobulins of various mammalian species. Scandinavian journal of immunology, 37(4), 399–405. Retrieved from http://www.ncbi.nlm.nih.gov/pubmed/8469922 [PubMed: 8469922]

Didar TF, & Tabrizian M (2010). Adhesion based detection, sorting and enrichment of cells in microfluidic Lab-on-Chip devices. Lab on a chip, 10(22), 3043–53. doi:10.1039/c0lc00130a [PubMed: 20877893]

Draper JS, Pigott C, Thomson J. a, & Andrews PW (2002). Surface antigens of human embryonic stem cells: changes upon differentiation in culture. Journal of anatomy, 200(Pt 3), 249–58. Retrieved from http://www.pubmedcentral.nih.gov/articlerender.fcgi?artid=1570685&tool=pmcentrez&rendertype=abstract [PubMed: 12033729]

Eiges R, Schuldiner M, Drukker M, Yanuka O, Itskovitz-Eldor J, & Benvenisty N (2001). Establishment of human embryonic stem cell-transfected clones carrying a marker for undifferentiated cells. Current biology : CB, 11(7), 514–8. Retrieved from http://www.ncbi.nlm.nih.gov/pubmed/11413002 [PubMed: 11413002]

Emre N, Vidal JG, Elia J, O'Connor ED, Paramban RI, Hefferan MP, … Carson CT (2010). The ROCK inhibitor Y-27632 improves recovery of human embryonic stem cells after fluorescence-activated cell sorting with multiple cell surface markers. PloS one, 5(8), e12148. doi:10.1371/journal.pone.0012148 [PubMed: 20730054]

Flanagan L. a, Lu J, Wang L, Marchenko S. a, Jeon NL, Lee AP, & Monuki ES (2008). Unique dielectric properties distinguish stem cells and their differentiated progeny. Stem cells (Dayton, Ohio), 26(3), 656–65. doi:10.1634/stemcells.2007-0810

Author Manuscript Author Manuscript Author Manuscript Author Manuscript

Fong CY, Peh GSL, Gauthaman K, & Bongso A (2009). Separation of SSEA-4 and TRA-1–60 labelled undifferentiated human embryonic stem cells from a heterogeneous cell population using magnetic-activated cell sorting (MACS) and fluorescence-activated cell sorting (FACS). Stem cell reviews, 5(1), 72–80. doi:10.1007/s12015-009-9054-4

Fong C-Y, Gauthaman K, & Bongso A (2010). Teratomas from pluripotent stem cells: A clinical hurdle. Journal of cellular biochemistry, 111(4), 769–81. doi:10.1002/jcb.22775 [PubMed: 20665544]

Gleghorn JP, Pratt ED, Denning D, Liu H, Bander NH, Tagawa ST, … Kirby BJ (2010). Capture of circulating tumor cells from whole blood of prostate cancer patients using geometrically enhanced differential immunocapture (GEDI) and a prostate-specific antibody. Lab on a Chip, 10, 27–29. Retrieved from 10.1039/B917959C [PubMed: 20024046]

Gu B, Zhang J, Wang W, Mo L, Zhou Y, Chen L, … Zhang M (2010). Global expression of cell surface proteins in embryonic stem cells. PloS one, 5(12), e15795. doi:10.1371/journal.pone.0015795 [PubMed: 21209962]

Hewitt Z, Forsyth NR, Waterfall M, Wojtacha D, Thomson a J., & McWhir J (2006). Fluorescence-activated single cell sorting of human embryonic stem cells. Cloning and stem cells, 8(3), 225–34. doi:10.1089/clo.2006.8.225 [PubMed: 17009898]

Holm F (2012). Cryopreservation of Human Embryonic Stem Cells and Induced Pluripotent Stem Cells. In Ye K & Jin S (Eds.), Human Embryonic and Induced Pluripotent Stem Cells (pp. 85–90). Totowa, NJ: Humana Press. doi:10.1007/978-1-61779-267-0

Hwang NS, Varghese S, & Elisseeff J (2007). Chapter 24: Cartilage Tissue Engineering - Directed Differentiation of Embryonic Stem Cells in Three-Dimensional Hydrogel Culture. In Stem Cell Assays (Vol. 407, pp. 351–373).

Jabart EB, Balakrishnan KR, & Sohn LL (n.d.). Label-Free Microfluidic Techniques to Isolate and Screen Single Stem Cells. In Stem Cells and Tissue Engineering, 2nd version. World Scientific Publishing, Inc.

Lindström S, & Andersson-Svahn H (2010). Overview of single-cell analyses: microdevices and applications. Lab on a Chip, 10, 3363–3372. Retrieved from http://www.ncbi.nlm.nih.gov/pubmed/20967379 [PubMed: 20967379]

Liu Y, Judd K, & Lakshmipathy U (2013). Chapter 21: Stable Transfection Using Episomal Vectors to Create Modified Human Embryonic Stem Cells. In Lakshmipathy U & Vemuri MC (Eds.), Pluripotent Stem Cells (Vol. 997, pp. 263–272). Totowa, NJ: Humana Press. doi:10.1007/978-1-62703-348-0

Liu Y, Lakshmipathy U, Ozgenc A, Thyagarajan B, Lieu P, Fontes A, … Chesnut JD (2010). hESC Engineering by Integrase-Mediated Chromosomal Targeting. In Turksen K (Ed.), Human Embryonic Stem Cell Protocols (Vol. 584, pp. 229–268). Totowa, NJ: Humana Press. doi:10.1007/978-1-60761-369-5

Mantel C, Guo Y, Lee MR, Kim M-K, Han M-K, Shibayama H, … Broxmeyer HE (2007). Checkpoint-apoptosis uncoupling in human and mouse embryonic stem cells: a source of karyotpic instability. Blood, 109(10), 4518–27. doi:10.1182/blood-2006-10-054247 [PubMed: 17289813]

McCarty OJT, Jadhav S, Burdick MM, Bell WR, & Konstantopoulos K (2002). Fluid shear regulates the kinetics and molecular mechanisms of activation-dependent platelet binding to colon carcinoma cells. Biophysical journal, 83, 836–848. doi:10.1016/S0006-3495(02)75212-0 [PubMed: 12124268]

Mittal S, Wong IY, Deen WM, & Toner M (2012). Antibody-functionalized fluid-permeable surfaces for rolling cell capture at high flow rates. Biophysical journal, 102(4), 721–30. doi:10.1016/j.bpj.2011.12.044 [PubMed: 22385842]

Murthy SK, Sin A, Tompkins RG, & Toner M (2004). Effect of flow and surface conditions on human lymphocyte isolation using microfluidic chambers. Langmuir The Acs Journal Of Surfaces And Colloids, 20, 11649–11655. Retrieved from http://www.ncbi.nlm.nih.gov/pubmed/15595794 [PubMed: 15595794]

Myung JH, Launiere C. a, Eddington DT, & Hong S (2010). Enhanced tumor cell isolation by a biomimetic combination of E-selectin and anti-EpCAM: implications for the effective separation

Author Manuscript Author Manuscript Author Manuscript Author Manuscript

of circulating tumor cells (CTCs). Langmuir : the ACS journal of surfaces and colloids, 26(11), 8589–96. doi:10.1021/la904678p [PubMed: 20155985]

Nagrath S, Sequist LV, Maheswaran S, Bell DW, Irimia D, Ulkus L, … Toner M (2007). Isolation of rare circulating tumour cells in cancer patients by microchip technology. Nature, 450, 1235–1239. Retrieved from http://www.pubmedcentral.nih.gov/articlerender.fcgi?artid=3090667&tool=pmcentrez&rendertype=abstract [PubMed: 18097410]

Plouffe BD, Kniazeva T, Mayer JE, Murthy SK, & Sales VL (2009). Development of microfluidics as endothelial progenitor cell capture technology for cardiovascular tissue engineering and diagnostic medicine. The FASEB journal official publication of the Federation of American Societies for Experimental Biology, 23, 3309–3314. doi:10.1096/fj.09-130260 [PubMed: 19487310]

Pratt ED, Huang C, Hawkins BG, Gleghorn JP, & Kirby BJ (2011). Rare Cell Capture in Microfluidic Devices. Chemical engineering science, 66(7), 1508–1522. doi:10.1016/j.ces.2010.09.012 [PubMed: 21532971]

Qiu D, Xiang J, Li Z, Krishnamoorthy A, Chen L, & Wang R (2008). Profiling TRA-1–81 antigen distribution on a human embryonic stem cell. Biochemical and biophysical research communications, 369(2), 735–40. doi:10.1016/j.bbrc.2008.02.102 [PubMed: 18313397]

Quinlan LR (2006). Phosphoinositides, Inositol Phosphates, and Phospholipase C in Embryonic Stem Cells. In Methods in Molecular Biology: Embryonic Stem Cell Protocols (Vol. 329, pp. 127–149).

Reverberi R, & Reverberi L (2007). Factors affecting the antigen-antibody reaction. Blood transfusion = Trasfusione del sangue, 5(4), 227–40. doi:10.2450/2007.0047-07 [PubMed: 19204779]

Schriebl K, Satianegara G, Hwang A, Tan HL, Fong WJ, Yang HH, … Choo A (2012). Selective Removal of Undifferentiated Human Embryonic Stem Cells Using Magnetic Activated Cell Sorting Followed by a Cytotoxic Antibody, 18. doi:10.1089/ten.tea.2011.0311

Sekine K, Revzin A, Tompkins RG, & Toner M (2006). Panning of multiple subsets of leukocytes on antibody-decorated poly(ethylene) glycol-coated glass slides. Journal of Immunological Methods, 313, 96–109. Retrieved from http://www.ncbi.nlm.nih.gov/pubmed/16822521 [PubMed: 16822521]

Sidhu KS, & Tuch BE (2006). Cell Lines by FACS Sorting and Their Characterization, 69, 61–69.

Singh A, Suri S, Lee T, Chilton JM, Cooke MT, Chen W, … García AJ (2013). Adhesion strength-based, label-free isolation of human pluripotent stem cells. Nature methods, 10(5), 438–44. doi:10.1038/nmeth.2437 [PubMed: 23563795]

Stewart MH, Bossé M, Chadwick K, Menendez P, Bendall SC, & Bhatia M (2006). Clonal isolation of hESCs reveals heterogeneity within the pluripotent stem cell compartment. Nature …, 3(10). doi:10.1038/NMETH939

Stott SL, Hsu C-H, Tsukrov DI, Yu M, Miyamoto DT, Waltman BA, … Toner M (2010). Isolation of circulating tumor cells using a microvortex-generating herringbone-chip. Proceedings of the National Academy of Sciences, 107, 18392–18397. doi:10.1073/pnas.1012539107

Tárnok A, Ulrich H, & Bocsi J (2010). Phenotypes of stem cells from diverse origin. Cytometry Part A the journal of the International Society for Analytical Cytology, 77, 6–10. Retrieved from http://www.ncbi.nlm.nih.gov/pubmed/20024907 [PubMed: 20024907]

Thomson J. a. (1998). Embryonic Stem Cell Lines Derived from Human Blastocysts. Science, 282(5391), 1145–1147. doi:10.1126/science.282.5391.1145 [PubMed: 9804556]

Toh Y-C, & Voldman J (2011). Fluid shear stress primes mouse embryonic stem cells for differentiation in a self-renewing environment via heparan sulfate proteoglycans transduction. The FASEB journal official publication of the Federation of American Societies for Experimental Biology, 25, 1208–1217. Retrieved from http://www.pubmedcentral.nih.gov/articlerender.fcgi?artid=3058703&tool=pmcentrez&rendertype=abstract [PubMed: 21183594]

Velugotla S, Pells S, Mjoseng HK, Duffy CRE, Smith S, De Sousa P, & Pethig R (2012). Dielectrophoresis based discrimination of human embryonic stem cells from differentiating derivatives. Biomicrofluidics, 6(4), 44113. doi:10.1063/1.4771316 [PubMed: 24339846]

Bronner Vered, Tabul Moran, B. T (2009). Rapid Screening and Selection of Optimal Antibody Captureing Agents Using the ProteOn XPR36 Protein Interaction Array System. Bio-Rad Laboratories.

Author Manuscript Author Manuscript Author Manuscript Author Manuscript

Wang S, Liu K, Liu J, Yu ZT-F, Xu X, Zhao L, … Tseng H-R (2011). Highly efficient capture of circulating tumor cells by using nanostructured silicon substrates with integrated chaotic micromixers. Angewandte Chemie International Edition, 50, 3084–3088. doi:10.1002/anie.201005853 [PubMed: 21374764]

Wang S, Wang H, Jiao J, Chen K-J, Owens GE, Kamei K, … Tseng H-R (2009). Three-dimensional nanostructured substrates toward efficient capture of circulating tumor cells. Angewandte Chemie International Edition, 48, 8970–8973. Retrieved from http://www.pubmedcentral.nih.gov/articlerender.fcgi?artid=2878179&tool=pmcentrez&rendertype=abstract [PubMed: 19847834]

Wang X, Chen S, Kong M, Wang Z, Costa KD, Li R. a, & Sun D (2011). Enhanced cell sorting and manipulation with combined optical tweezer and microfluidic chip technologies. Lab on a chip, 11(21), 3656–62. doi:10.1039/c1lc20653b [PubMed: 21918752]

Zhao W, Ji X, Zhang F, Li L, & Ma L (2012). Embryonic stem cell markers. Molecules (Basel, Switzerland), 17(6), 6196–236. doi:10.3390/molecules17066196

Zheng X, Cheung LS-L, Schroeder J. a, Jiang L, & Zohar Y (2011). Cell receptor and surface ligand density effects on dynamic states of adhering circulating tumor cells. Lab on a chip, 11(20), 3431–9. doi:10.1039/c1lc20455f [PubMed: 21853194]

Author Manuscript Author Manuscript Author Manuscript Author Manuscript

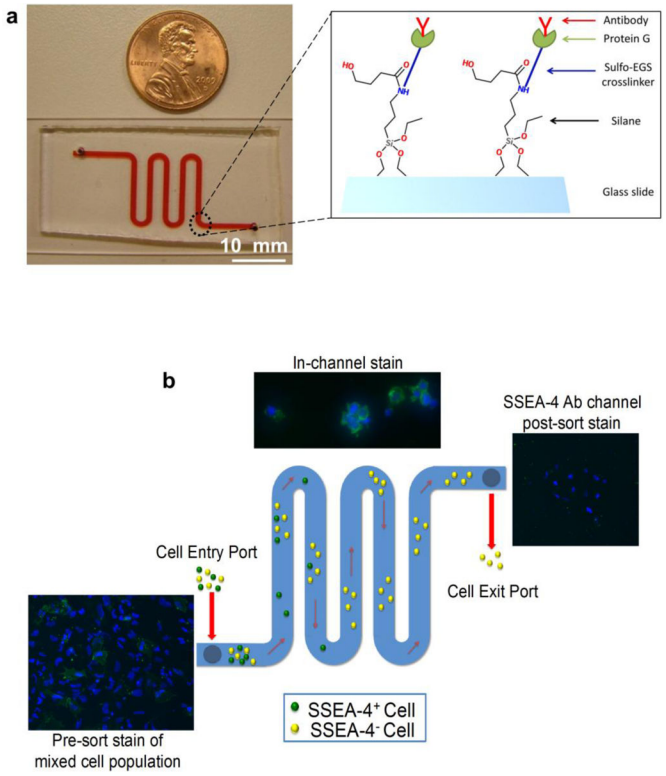

Fig.1.

a) Image of the serpentine channel and inset of functionalization strategy (see Device functionalization). The (94 mm × 1 mm × 80 μm) (L × W × H) channel is cored at both ends for inlet and outlet ports. b) A schematic of the device method, using an anti-SSEA-4-functionalized-antibody channel as an example (although any antibody of choice can be used). A mixed population of cells is added at the inlet port. The outlet port is connected to a syringe pump via plastic tubing. As the cells traverse the device, SSEA-4^{+} cells become bound to the functionalized antibodies and SSEA-4^{-} cells pass through the device and are collected in a syringe. At the end of the run, the device is washed thoroughly with fresh cell media, corresponding to the appropriate cell types (see Materials and Methods: Cell Culture).Control cells (i.e. those not injected into the channel) and uncaptured cells passed are plated, allowed to adhere to Matrigel-coated plates, fixed, and immunostained for either SSEA-4^{+} or OCT4^{+}. Captured cells are stained and imaged in-channel. The percentage of SSEA-4^{+} or OCT4^{+} captured and not captured cells is then determined

Author Manuscript Author Manuscript Author Manuscript Author Manuscript

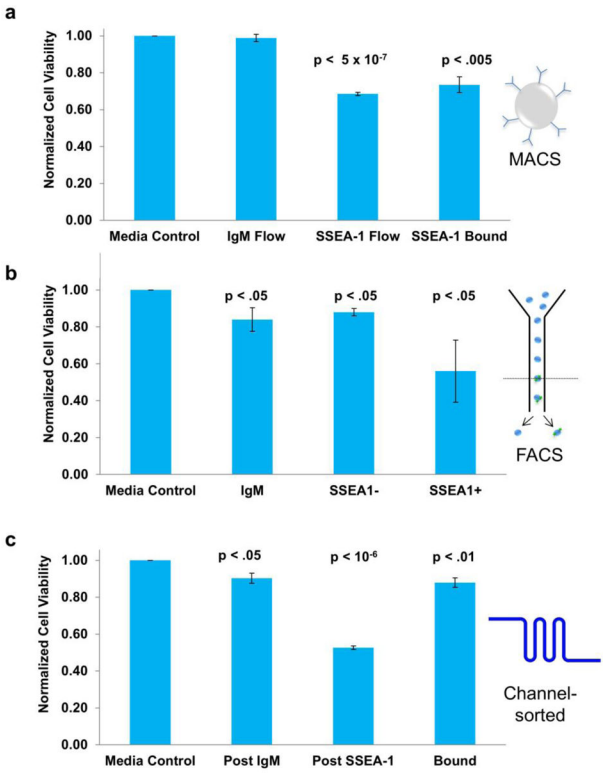

Fig.2.

Comparison of cell viability using MACS, FACS, and our microfluidics-based method. J1 mESCs cells were employed in all three methods and assayed for viability using a Live/Dead® assay. Average values from 3 independent experiments were normalized to results from cells that were maintained in media. Error bars corresponds to standard error. a) MACS: Assayed cells were collected under the following conditions: anti-IgM Microbeads (flow-through) and anti-SSEA-1 Microbeads (both flow-through and bound fractions). b) FACS: Assayed cells were those incubated with anti-IgM and those positively and negatively sorted for SSEA-1. c) Microfluidic isolation: Assayed cells were those that traversed anti-IgM- or anti-SSEA-1-functionalized antibody channels, as well as bound cells recovered from anti-SSEA-1-functionalized channels

Author Manuscript Author Manuscript Author Manuscript Author Manuscript

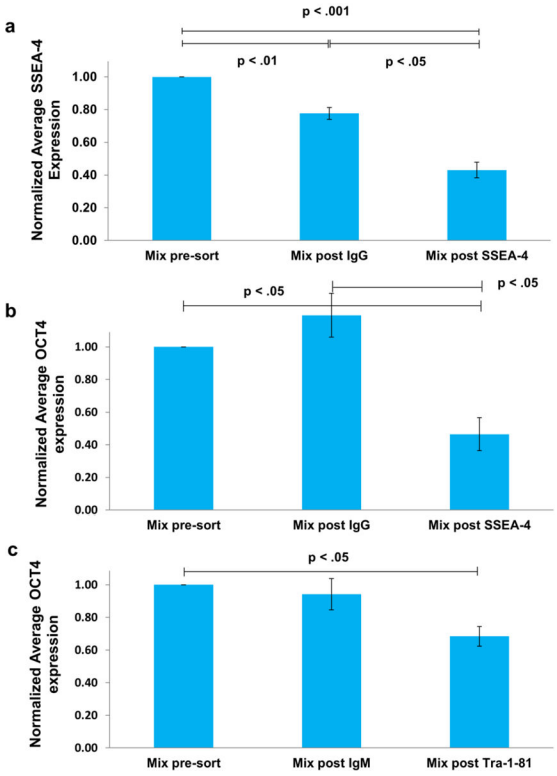

Fig.3.

a) Normalized average SSEA-4 expression for microchannel runs. A 4:1 ratio of hESCs to A549 were passed through either anti-IgG or anti-SSEA-4-functionalized channels. Control cells (those that do not run through any channel), and cells recovered after traversing either through anti-IgG channels or anti-SSEA-4 channels were plated and stained for the undifferentiated hESC marker, SSEA-4. Average values from 5 independent experiments were normalized to the fraction of SSEA-4 positive control cells. Error bars represent standard error. b) Normalized average OCT-4 expression for microchannel runs. A 4:1 ratio of hESCs to A549 cells were passed through either anti-IgG or anti-SSEA-4-functionalized channels. Control cells, cells recovered after traversing through anti-IgG channels, and cells recovered after passing through anti-SSEA-4 channels were plated and stained for the undifferentiated hESC antigen, OCT4. Average values from 4 independent experiments were normalized to the fraction of $SSEA\text{-}4^{+}$ control cells. Error bars represent standard error. c) Normalized average OCT4 expression for microchannel runs. A 4:1 ratio of hESCs to A549s was passed through either anti-IgM or anti-Tra-1–81-functionalized channels. Control cells, cells recovered after traversing through anti-IgM channels, and cells recovered after passing through anti-Tra-1–81 channels were plated and stained for the undifferentiated hESC marker, OCT4. Average values from 3 independent experiments were normalized to the fraction of $OCT4^{+}$ cells in the control cells. Error bars represent standard error